Kim et al. Micro and Nano Systems Letters (2024) 12:1
https://doi.org/10.1186/s40486-023-00192-9

Micro and Nano Systems Letters

LETTER

Open Access

PCB-based digital microfluidic platform for droplet mixing on an open surface

Hyunwoo Kim[1], Sang Kug Chung[1*] and Jeongmin Lee[2*]

Abstract

This paper presents a digital microfluidic (DMF) platform based on a printed circuit board (PCB) for droplet mixing. Mixing droplets without a top cover plate is important for bio-chemical analysis. For this reason, a more efficient mixing method is required especially for mixing a viscous liquid droplet in an open surface. Here, to improve the performance of droplet mixing, we propose the integration of an acoustically oscillating bubble to an electrowetting-on-dielectric (EWOD) chip, which can generate microstreaming inside the droplet. Firstly, an EWOD chip integrated with through-holes for bubble trapping was designed and fabricated through PCB fabrication. This PCB manufacturing technology helps to place more electrodes in the limited chip size. Secondly, we developed the custom-made circuit and interface to individually control multiple actuators (including EWOD actuation and acoustic excitation). Finally, an operation test was conducted to evaluate the capability of not only droplet transportation but also mixing on an open surface. The proposed PCB-based DMF platform for bubble-induced droplet mixing was experimentally verified and expected to make DMF chips more efficient when used for clinical point-of-care diagnostic applications.

Keywords Digital microfluidic platform, Printed circuit board, Through-hole, Droplet, Electrowetting

Introduction

A digital microfluidic (DMF) platform is a liquid-handling tool for the transportation, merging, separating, and mixing of nano-to-microscale droplets. The DMF platforms normally use electrowetting-on-dielectric (EWOD) actuation with an electrode array deposited with a hydrophobic insulator [1, 2] because of its rapid response and controllability. These DMF platforms have been exploited to manipulate a small amount of biological fluid (e.g., blood, lymph) and reagents [3–5] in point-of-care testing and diagnosis applications. To expand the usefulness of the DMF platform for biological applications, as many samples as possible should be processed in a limited amount of cost and time. To achieve this, the DMF platform needs to have a low-cost fabrication technique for EWOD actuators and an efficient mixing capability of droplets.

DMF platform should be able to individually control multiple droplets at the same time. Thus, a system must be established where electrodes are not only connected to a control circuit but also provided with electrical potential from the control circuit [6]. Many researchers fabricate DMF chips, which have numerous electrodes connected to a control circuit, through the microfabrication process to efficiently arrange the electrodes and wiring in a limited space on glass or silicon substrates [7, 8]. However, the high cost of microfabrication acts as a major barrier limiting user access to the device in terms of research and commercialization. The cost issue becomes more pronounced when controlling biochemical droplets leads to issues such as biofouling [9], cross-contamination [10], dielectric breakdown [11], or when a different electrode pattern is required. On the other hand, printed circuit board (PCB) can be a better option

*Correspondence:
Sang Kug Chung
skchung@mju.ac.kr
Jeongmin Lee
jmlee@microsystems.co.kr
[1] Department of Mechanical Engineering, Myongji University, Yongin 17058, Republic of Korea
[2] Microsystems, Inc., Yongin 17058, Republic of Korea

to reduce the fabrication cost of microscale electrode patterns. In addition, with through-holes that provide electrical connections between the top, bottom, and inner electrode layers of the PCB, more electrodes can be densely arranged in a certain space. For this reason, several research groups have concentrated on the development of PCB-based DMF platforms for droplet manipulation [12], nitrite sensing [13], and DNA analysis [14].

DMF platform is recently required to mix droplets quickly. The process of analyzing a biochemical sample consists of transportation, separation, mixing, and concentration, among which the mixing step accounts for the largest portion of the total processing time [15–17]. However, at the microscale, the Reynolds number is low, and viscous forces dominate. As a result, the mixing of fluids is heavily reliant on molecular diffusion, especially in highly viscous droplets such as blood or other body fluids, which naturally mix much more slowly [18, 19]. For this reason, the DMF platform needs to have the ability to improve the droplet mixing. Some research groups have utilized droplet transportation using sequential EWOD actuation [20], droplet oscillation using AC-EWOD actuation [21, 22], droplet oscillation using acoustic excitation [15], and surface acoustic waves [23] to facilitate the internal flow of droplets.

In previous studies, research on a PCB-based DMF platform has been conducted, aimed to transport droplets individually and improve droplet mixing. Alistar et al. [24] and Umapathi et al. [25] developed a PCB-based DMF platform with hundreds of electrodes, where droplet mixing has been achieved by repeating droplet transportation using EWOD actuation. However, there was a risk of the unwanted droplet merging in a confined space. Won et al. [26] proposed a PCB-based DMF platform which perform droplet transportation and mixing by combining EWOD actuation and acoustic bubbles, respectively. Although the method of utilizing acoustic bubbles has been experimentally proven to enhance mixing efficiency of droplets, the requirement to directly inject bubbles into the droplets for the mixing process is considered a disadvantage in terms of convenience.

In this paper, we propose a PCB-based DMF platform that utilizes naturally trapped acoustic bubbles to improve droplet mixing. This platform also exploits acoustically excited bubbles to improve droplet mixing and EWOD actuation to transport multiple droplets simultaneously. Especially, through-holes in an EWOD chip are strategically utilized not only to realize the connectivity between electrodes and control circuits but also to provide space for bubble trapping. The proposed DMF platform consists of an EWOD chip, driver board, and software. Figure 1 is a schematic diagram of the droplet manipulation process on the EWOD chip. Figure 1b1, b2 shows that two different biochemical droplets are transported to the center and merged by EWOD actuation on the chip. When the merged droplet arrives at the mixing zone, a bubble is naturally trapped in the structure of the EWOD chip, as demonstrated in Fig. 1b3. When an acoustic excitation is applied corresponding to the resonant frequency of the generated bubble, the bubble oscillates and simultaneously microstreaming occurs. Finally, mixing within the droplet is enhanced, as shown in Fig. 1b4.

Theoretical background

The proposed DMF platform utilizes an EWOD actuation to transport droplets. Electrowetting, more correctly EWOD, is a technology that electrically controls the interfacial tension of two fluids [27, 28]. When an electrical potential is applied between the conductive droplet and electrode covered by a hydrophobic insulator, electrical charges inside the droplet are accumulated around a triple contact line (TCL) because current cannot flow through the dielectric layer. As a result, the contact angle of the droplet is reduced because of the change in interfacial tension, and the droplet spreads on the electrode as shown in Fig. 2b. The relationship between the changed contact angle and the applied voltage can be explained by the Lippmann-Young equation, which is derived from the Lippmann equation using the parallel plate capacitance formula as follows [29, 30].

$$\cos\theta = \cos\theta_e + \frac{\varepsilon_0 \varepsilon_d V}{2\gamma t_d} \tag{1}$$

where θ is the contact angle at an applied voltage V, θ_e is the equilibrium contact angle at V = 0 V, ε_0 is the permittivity of the vacuum, ε_d is the permittivity of the dielectric layer, γ is the interfacial tension between the conductive liquid and the surrounding fluid, and t_d is the thickness of the dielectric layer. For more information, refer to other related papers [29, 31].

Device design

The proposed DMF platform consists of the EWOD chip, driver board, and software. The EWOD chip was designed not only to transport multiple droplets in parallel but also to promote droplet mixing. A four-layer PCB with dimensions of 82 × 53 × 1 mm^3, the EWOD chip was manufactured using a PCB fabrication process as shown in Fig. 3. The chip contains an electrode array for the EWOD actuation, through-holes for intentionally trapping bubbles, and pins for connection to the driver board, as shown in Fig. 3(b, c). The dimension of the electrode array is shown in Fig. 4a. A circular hole with a diameter of 0.4 mm is placed at the center of each electrode, which is used as space for bubble trapping, as shown in

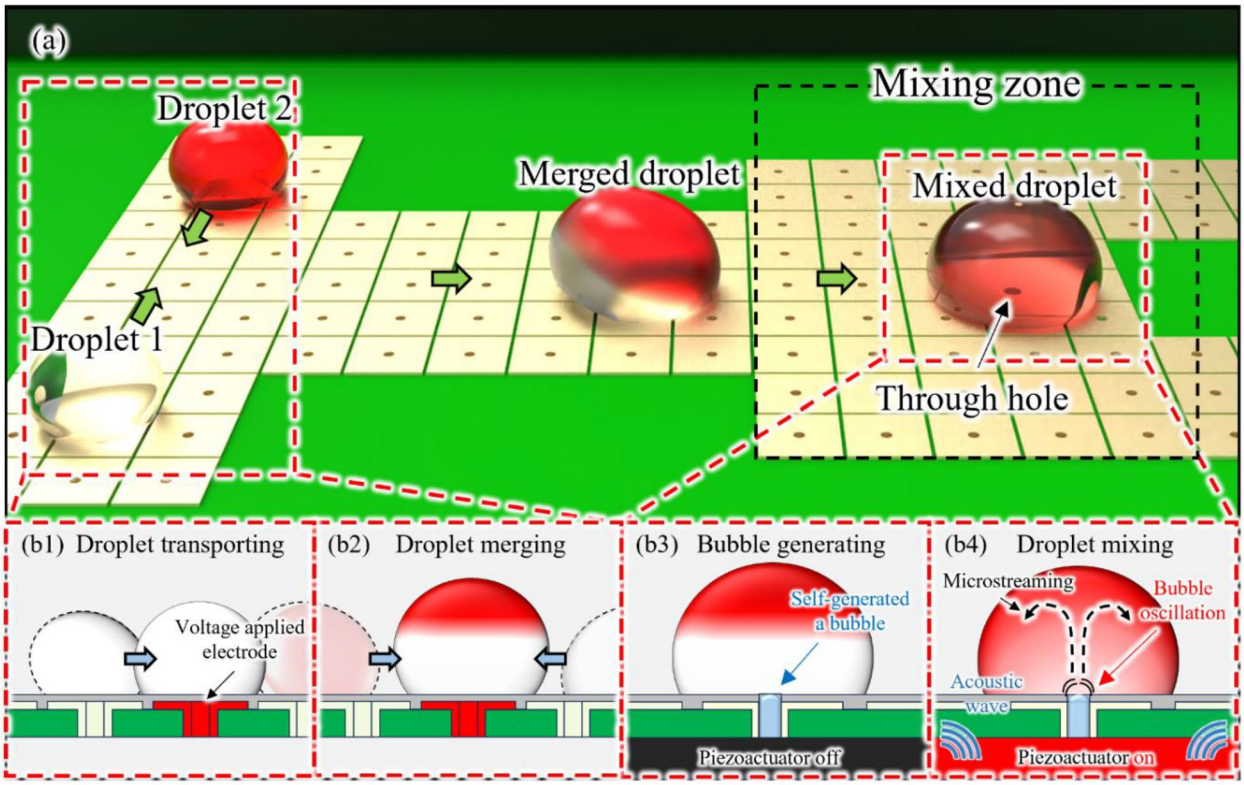

Fig. 1 **a** Schematic diagram of droplet manipulation process on the EWOD chip; (**b1**) Droplet transportation by EWOD actuation; (**b2**) Merging of two droplets with different properties; (**b3**) When the droplet is positioned over the hole, a bubble is naturally trapped; (**b4**) Droplet mixing facilitated by microstreaming, generated through the oscillation of the bubble excited by a piezoactuator

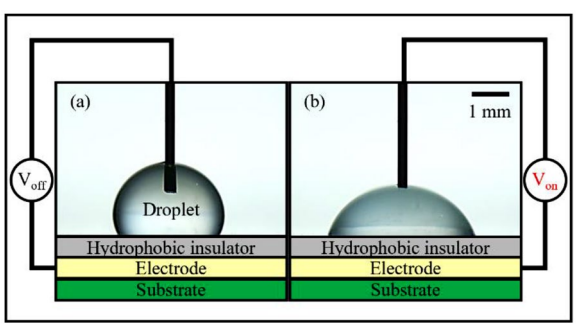

Fig. 2 Schematic diagram of electrowetting (EW): **a** Before applying voltage between a droplet and electrode; **b** The droplet spreading after applying voltage

Fig. 4b. In addition, these through-holes provide an electrical connection between the top and bottom layers of the board. The electrodes and pins are connected by copper wires on both sides and two inner layers of the PCB. There are 244 pins on both sides of the PCB, with a pitch of 0.6 mm for connection to the driver board.

From the inspiration of [24], the driver board was designed to amplify and transmit driving signals in parallel to the electrodes of the EWOD chip. To achieve this, the board integrated a voltage amplification circuit that boosts 12 V_{dc} to a range of 0–350 V_{dc}. A commercial memory socket (87918–0301, Molex) was mounted on the board to connect with the EWOD chip. To control EWOD electrodes and communicate with software, the board is equipped with a microprocessor (ATMEGA8A-AU, Microchip Technology) and four 64-channel serial-to-parallel converters (HV507PG, Microchip Technology) which provide parallel voltage output. The driver board connects to the software via a USB-C cable and interfaces with the EWOD chip through the memory socket. For device stability, a short-circuit protection section was integrated into the driver board.

To provide easy and versatile operation of the DMF platform, the control software was built in the Java language and works in a Windows environment. The output voltage amplitude and the electrodes that the voltage is applied are determined by the software. The software adjusts the output voltage in 10 V_{dc} steps up to 350 V_{dc}. There are two ways to define which electrodes receive the voltage. In the first method, "Sequence mode", a voltage signal is applied to the electrodes for a

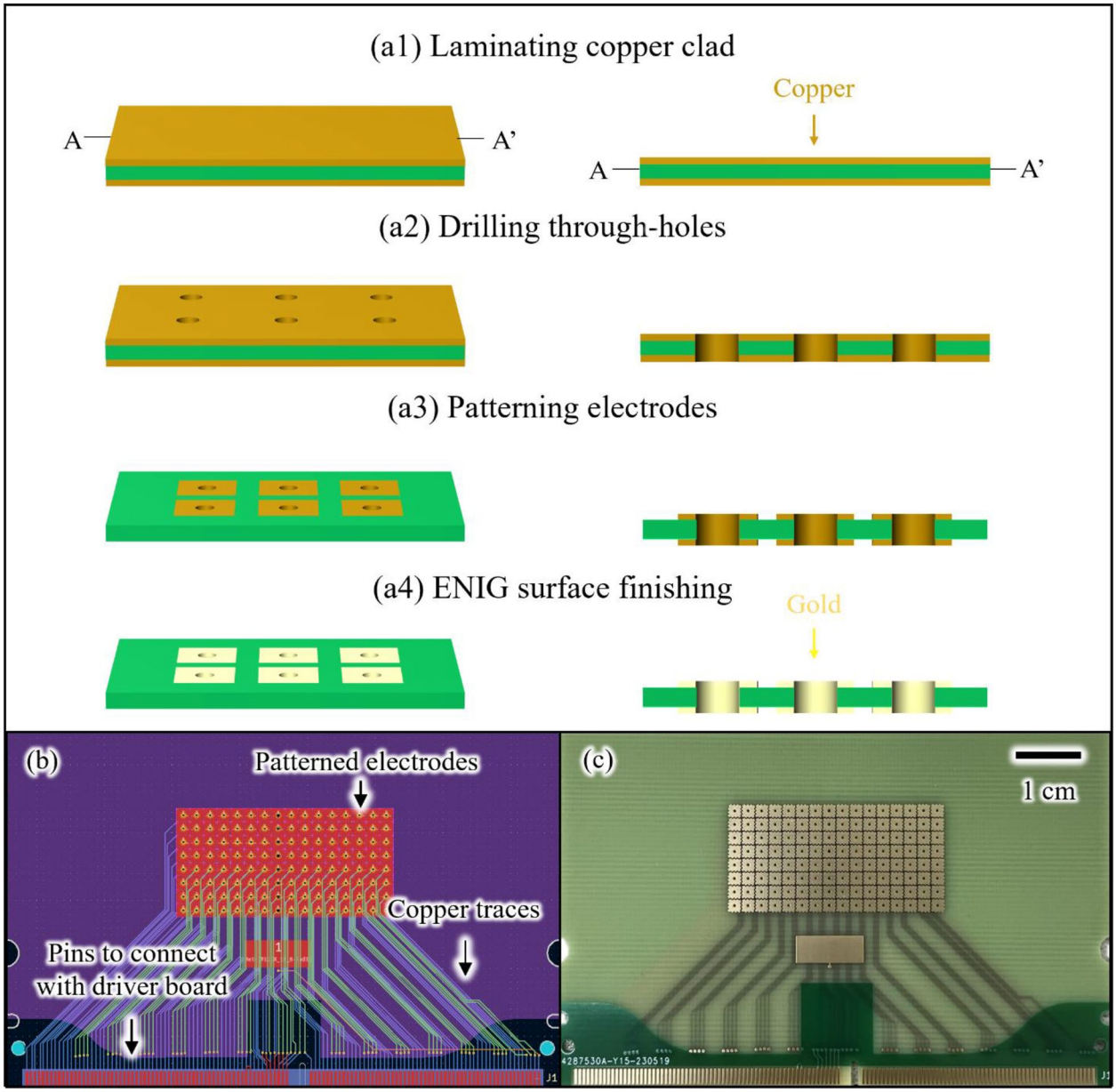

Fig. 3 **a** Schematic image of PCB-based EWOD chip manufacturing process; **b** Design of the EWOD chip with patterned electrodes, copper traces, and pins; **c** Physical image of the EWOD chip

duration ranging from 0 to 5000 ms. Each duration is called a "sequence," and up to 20 electrodes can be powered independently within a single sequence. A total of 10 sequential operations are available in the sequence mode, and the pin number of the memory connector is matched as the electrode number that is entered into the sequence. By utilizing this mode, it is possible to control droplets with different time conditions. In the second method, "Live mode," voltage is applied through buttons that correspond to individual electrodes. When a button is activated, voltage is applied to the corresponding electrode, allowing the user to control all electrodes in real-time.

Fabrication and experimental setup

To utilize EWOD actuation and acoustically excited bubbles, the deposition of a dielectric and hydrophobic layer is essential on the EWOD chip. To achieve this objective, two types of dielectric layers are considered. Parafilm M used with silicone oil can provide an effective

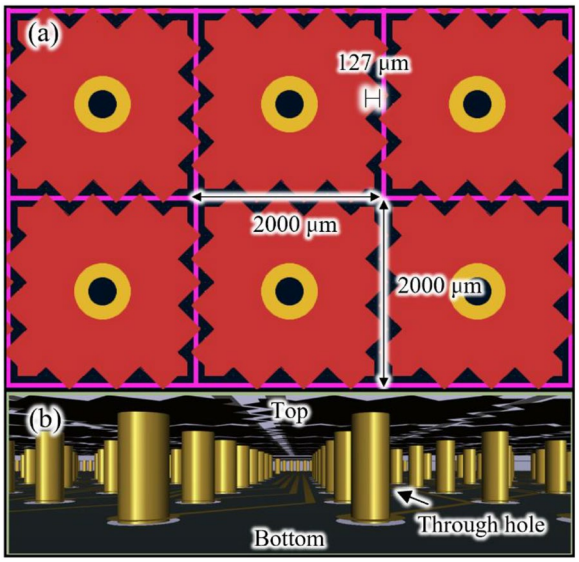

Fig. 4 **a** The design of electrode patterns on the EWOD chip; **b** Cross-sectional view of the EWOD chip, including the through-holes

environment for droplet transportation, ignoring the height and spacing of PCB electrodes that disturb droplet transportation. However, when bubbles are used to facilitate droplet mixing, there is a risk that the Parafilm will interfere with the oscillation of the bubbles by positioning between the droplets and the bubbles. Thus, Parylene C, which can be deposited while maintaining the shape of the through-holes, is used as an additional dielectric layer. In subsequent experiments, droplet transportation and mixing are experimentally verified using EWOD chips processed by these two methods.

Figure 5a shows the fabrication process of the EWOD chip A, which utilizes Parafilm as a dielectric layer. Initially, silicone oil 3 μL was applied for adhesion between the electrode and the Parafilm. Then the stretched Parafilm of 12 μm in thickness was attached, and silicone oil was applied to the parafilm for lubrication. Figure 5b shows the fabrication process of the EWOD chip B with Parylene as a dielectric layer. Using chemical vapor deposition (CVD), a Parylene layer of 2 μm in thickness was uniformly deposited while maintaining the shape of the through-holes. Then, an amorphous fluoropolymer layer (FluoroPel PFC1601V, CYTONIX) as a hydrophobic topcoat was spin-coated on the Parylene layer at 2000 rpm for 20 s. After deposition of the dielectric and hydrophobic layers, a piezoactuator (AB2072S, PUI Audio) with a diameter of 20 mm and a thickness of 0.45 mm was attached to the backside of the EWOD chip A and B. After the fabrication process completed, the EWOD chip B was photographed by a scanning electron microscope (SEM) (SNE-4500 M, Seron Technology) as shown in Fig. 6a. When a droplet is placed on the electrode of the chip B, a bubble is naturally trapped as shown in Fig. 6b.

A schematic diagram of the experimental setup is shown in Fig. 7. The required voltage for EWOD actuation is supplied by a power adapter and amplified by the driver board of the DMF platform. The amplified voltage signal is controlled by software. The piezoactuator

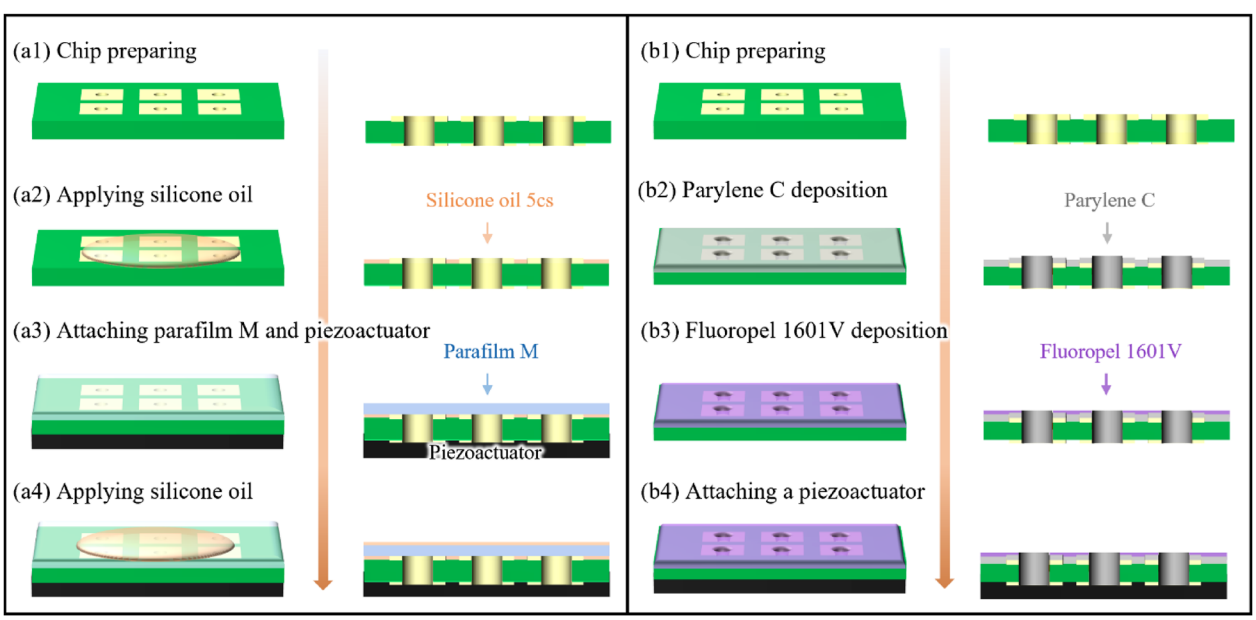

Fig. 5 Schematic images of the EWOD chip fabrication processes: **a** EWOD chip A using Parafilm M as dielectric layer and silicone oil as hydrophobic layer; **b** EWOD chip B using Parylene C as dielectric layer and FluoroPel as hydrophobic layer

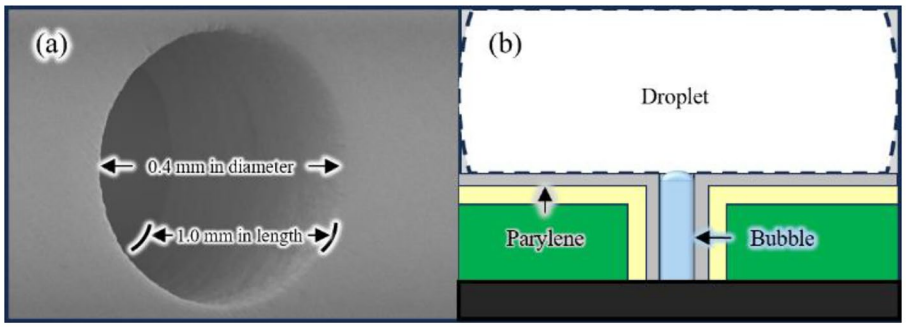

Fig. 6 **a** SEM image of the through-hole after the fabrication process is complete on the EWOD chip B; **b** Schematic image of a bubble naturally trapped in the through-hole

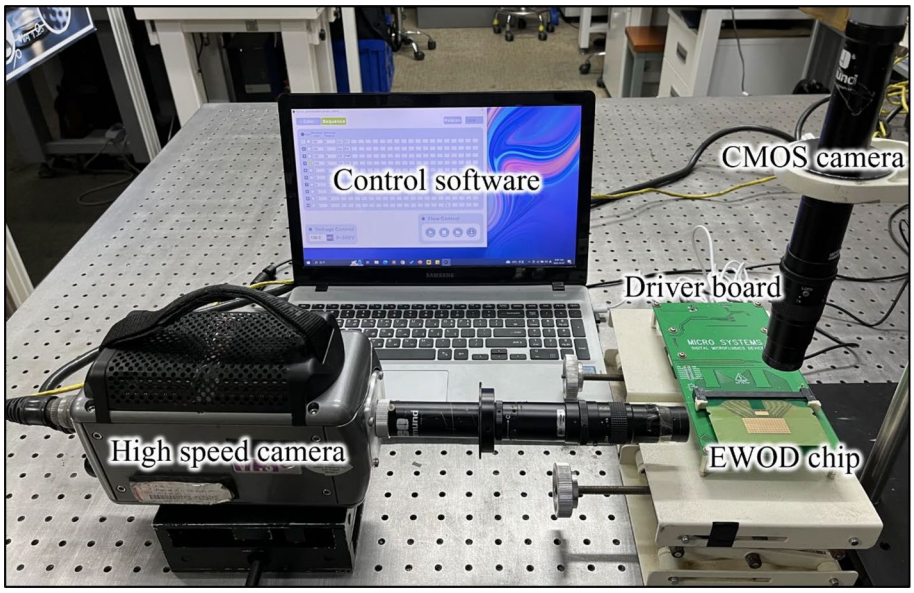

Fig. 7 Experimental setup to validate droplet transportation and mixing capabilities on the proposed DMF platform

attached to the EWOD chip is driven by a function generator (33210A, Agilent) and voltage amplifier (PZD700, Trek). All experiments are captured by a CMOS color camera (EO-1312C, Edmund Optics) and high-speed camera (Phantom Micro eX4, Vision Research). A detailed schematic diagram of the signals for the DMF platform operation is presented in Fig. 8.

Experimental results & discussion

A droplet contact angle measurement experiment was performed to verify the basic EWOD operation on the proposed DMF platform. For the experiment, a distilled water droplet of 15 μL in volume was placed on the electrode. When a electrical voltage was applied between the droplet and the electrode, the contact angle decreased by the EWOD actuation. The contact angle change was measured in the range of 0–350 V_{dc} using a contact angle goniometer (Smartdrop, Femtobiomed), and the average value was calculated from the results of three repeated experiments. The experimental results are shown in Fig. 9. For both EWOD chip A and B, the contact angle of the droplet decreased as the voltage increased. The contact angles of droplets on the chip A and B followed the Lippmann-Young equation up to 100 and 300 V_{dc}, respectively, but after these voltages contact angle saturation occurred. Within the voltage range of 0–350 V_{dc}, we found the maximum value of contact angle change was about 55° for the chip A and 65° for the chip B. This result shows that EWOD actuation on two different dielectric layers was fully operated, and sufficient contact angle change was achieved within the voltage range of the DMF platform. Normally, the relationship between the dielectric layer and contact angle change is inversely proportional according to Eq. (1).

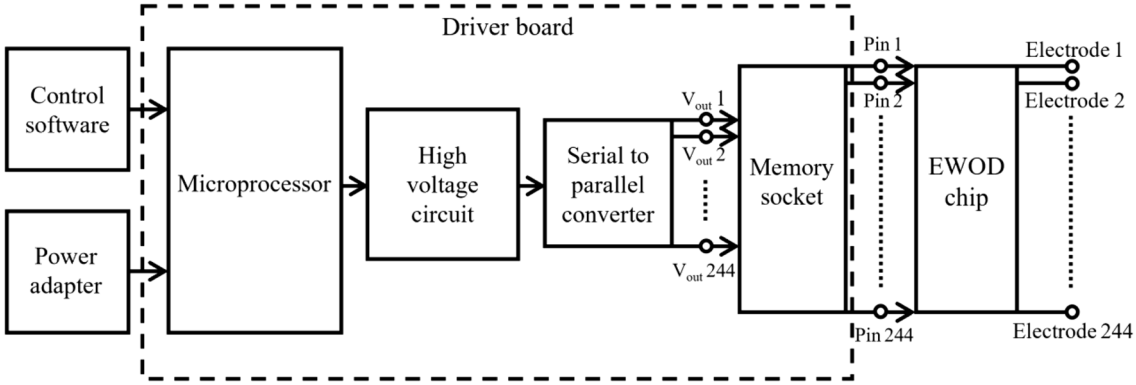

Fig. 8 Schematic diagram of activation signal flow on the DMF platform

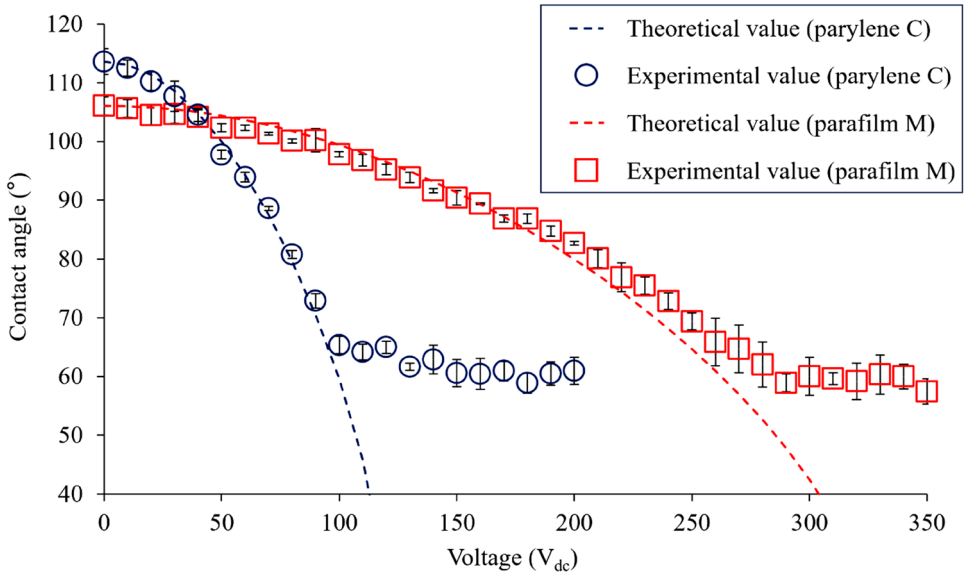

Fig. 9 Experimental results and theoretical values of contact angle measurement with applied voltage when Parylene C and Parafilm M are used as dielectric layers

Hence, for low-voltage operation of EWOD, the thickness is required to decrease. On the other hand, for reliable EWOD actuation with no dielectric breakdown, the thickness of the dielectric layer is needed to increase as the electric field applied to the dielectric layer lowers the dielectric strength of the layer. Considering the trade-off relationship between the performance and reliability of an EWOD actuator, a dielectric layer thickness and driving voltage should be optimized in future research.

Next, to investigate droplet transportation and threshold voltage for droplet transportation, droplet velocity was measured at different voltages on the EWOD chip A and B. For the experiment, a water droplet of 20 μL in volume was placed on the chips and a high electrical voltage was applied to the electrodes through control software. The droplet velocity was analyzed from the images captured using the CMOS camera, and the maximum velocity was calculated after 3 times of measurement. The result of the droplet velocity measurement is shown in Fig. 10. The experimental results show that on the EWOD chip A, the droplets start to move onto the electrodes when a voltage higher than 100 V_{dc} is applied. In contrast, at voltages lower than 100 V_{dc}, the droplets could not be positioned on the activated electrodes. The velocity increases with increasing voltage. At 100 V_{dc}, the droplet velocity was measured to be about 2.5 mm/s, and at 280 V_{dc} and above 40 mm/s. On the other hand, on the chip B, the droplet moved, but continuous movement was not possible. We suspect that the presence of a hole makes the droplet movement difficult.

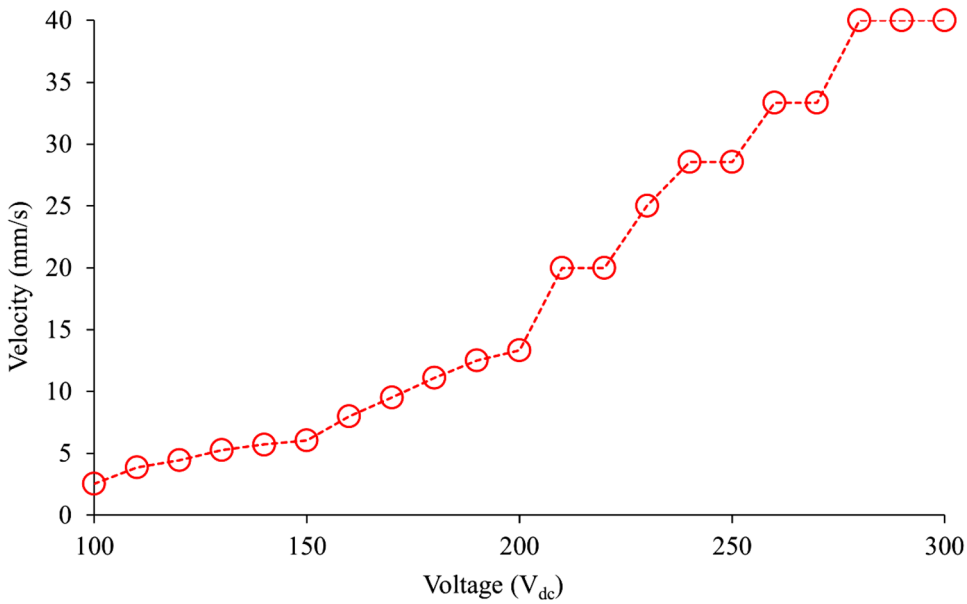

Fig. 10 Droplet velocity measurement result of 20 μL water with different voltage on the EWOD chip A

To verify the parallel control of droplets on the DMF platform, a multiple droplet transportation experiment was performed. For the experiment, five 20 μL water droplets were placed on the EWOD chip A as shown in Fig. 11a1. Then, a 300 V_{dc} voltage was applied at 100 ms intervals to sequentially transport the droplets. The experimental results show that the droplets sequentially transported to the applied electrodes as shown in Fig. 11a2, a3. This result confirmed that multiple droplets can be controlled individually on the DMF platform.

Flow visualization experiment was performed to validate the mixing facilitation method using an acoustic bubble. For the experiment, a 20 μL volume of water droplet with added 6 μm diameter fluorescent particles (FF1015-01, EBM) was placed on the EWOD chip A and B. The fluorescent particles inside the droplet were observed utilizing a 532 nm laser light source (MGL-H-532 nm, Changchun New Industries Optoelectronics Technology) and a high-speed camera. Figure 12 shows the image of the flow field inside the droplet, which was stacked using Startrails software. The white dots in Fig. 12 represent fluorescent particles. For the chip A, the Parafilm was positioned between the droplet and the bubble, as shown in Fig. 12a1. For the chip B, a tubular bubble (0.4 mm in diameter and 1 mm in length) was located directly at the bottom of the droplet, as shown in Fig. 12b1. Before the acoustic excitation was applied, there was no particle movement observed inside the droplet. When applying acoustic excitation in the frequency range of 0 to 10 kHz using a piezoactuator attached to the bottom of the chip, particle movement inside the droplet was not observed on the chip A, as shown in Fig. 12a2. On the other hand, for the chip B, when an acoustic excitation of 3.529 kHz was applied to the bubble, the bubble oscillated and microstreaming occurred inside the droplet, as shown in Fig. 12b2. The red arrows in Fig. 12b2 indicate the movement path of the fluorescent particles due to the microstreaming. The

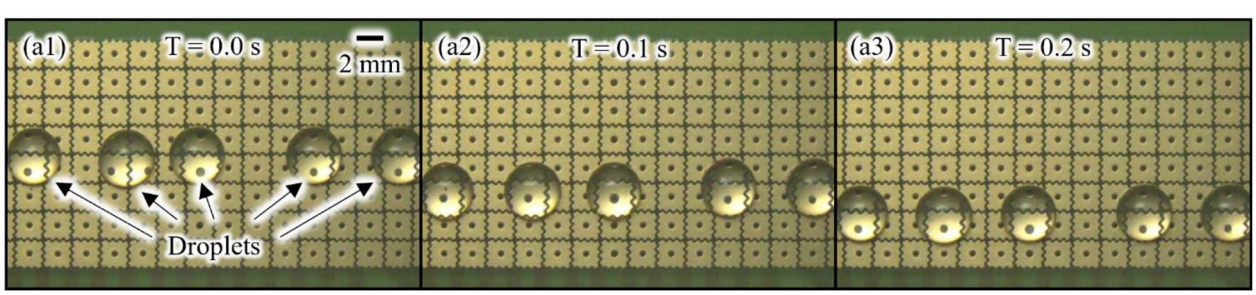

Fig. 11 Sequential snapshots of individual transportation of five 20 μL water droplets on the EWOD chip B using 300 V_{dc} voltage at 100 ms intervals

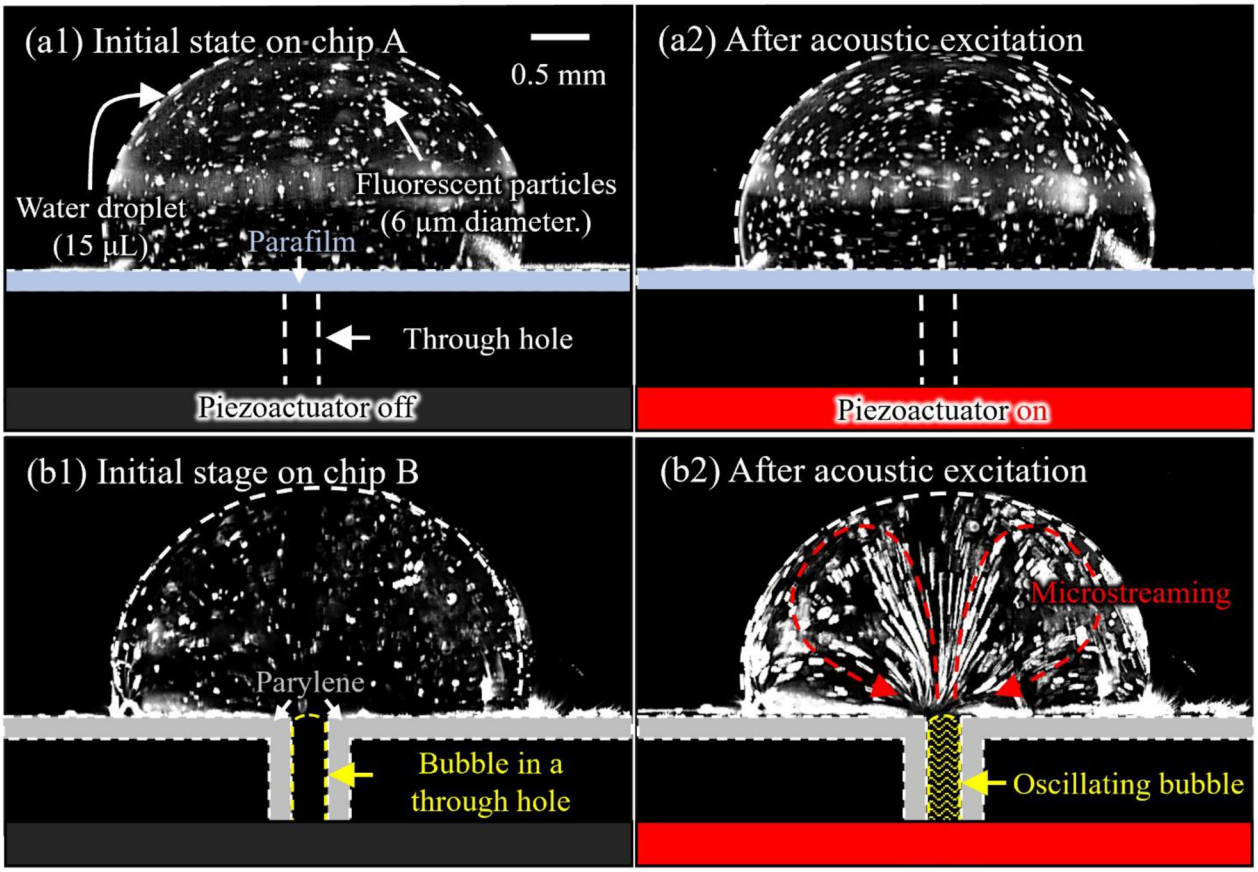

Fig. 12 Flow visualization with acoustic excitation at 3.529 kHz and 30 V_{pp} by piezoactuator: **a** The chip A cannot create the flow inside the droplet; **b** The chip B generates a microstreaming with an acoustically excited bubble (0.4 mm in diameter and 1 mm in length) in a through-hole of the PCB substrate

microstreaming generated by the bubble oscillation has a symmetrical shape, rising from the center of the bubble and falling from the boundary of the droplet, showing an overall circular shape. This result shows the feasibility that the proposed method was able to generate the internal flow in droplets and to mix droplet only if the PCB chip has holes.

In summary, two different dielectric layers were used to validate droplet transportation and mixing on the DMF platform. For the chip A, droplet transportation was possible, but mixing with bubbles was not successful. For the chip B, droplet mixing is possible but requires improvement for transportation. Future research direction involves improving droplet transportation in the chip B with holes and implementing a chip for both droplet transportation and mixing.

Conclusion

In this paper, we present a PCB-based DMF platform that utilizes EWOD actuation for droplet transportation and acoustically excited bubbles for droplet mixing. Firstly, we designed an EWOD chip that can transport and mix the droplets. In particular, the through-hole structure of the PCB has allowed to intentionally trap bubbles in through-holes, and the complex wiring of the electrodes has been solved simply. Subsequently, we developed a driver board and control software for efficient control of the EWOD chip. The driver board has a driving voltage range of 0–350 V_{dc}, and the software controls the platform in two modes for user convenience. Finally, to study the droplet movement and mixing feasibilities of the developed DMF platform, a performance test was conducted with two EWOD chips. Droplets were transported at 2 mm/s at 100 V_{dc} and 40 mm/s at 300 V_{dc}, and multiple droplets could be controlled individually with the proposed platform. Then, through flow visualization experiments, the feasibility of the flow inside droplets by a tubular bubble is experimentally verified. In future research, for comparison of mixing performances, liquids with different viscosities are additionally investigated. The proposed

DMF platform is expected to be utilized in the clinical diagnostic field due to a high accessibility and low cost.

Acknowledgements
Not applicable.

Author contributions
HK: conceptualization, data curation, formal analysis, investigation, methodology, software, visualization, writing—draft preparation. SKC: conceptualization, supervision, project administration, writing—review and editing. JL: conceptualization, methodology, supervision, writing—draft preparation, writing—review and editing. All authors read and approved the final manuscript.

Funding
Not applicable.

Availability of data and materials
All data generated or analyzed during this study are included in this published article [and its supplementary information files].

Declarations

Competing interests
The authors declare that they have no competing interests.

Received: 1 November 2023 Accepted: 12 December 2023
Published online: 03 January 2024

References

1. Pollack MG, Shenderov AD, Fair RB (2002) Electrowetting-based actuation of droplets for integrated microfluidics. Lab Chip 2:96–101. https://doi.org/10.1039/b110474h
2. Cho SK, Moon H, Kim CJ (2003) Creating, transporting, cutting, and merging liquid droplets by electrowetting-based actuation for digital microfluidic circuits. J Microelectromech Syst 12:70–80. https://doi.org/10.1109/JMEMS.2002.807467
3. Jebrail MJ, Bartsch MS, Patel KD (2012) Digital microfluidics: a versatile tool for applications in chemistry, biology and medicine. Lab Chip 12:2452–2463. https://doi.org/10.1039/c2lc40318h
4. Pollack MG, Pamula VK, Srinivasan V, Eckhardt AE (2011) Applications of electrowetting-based digital microfluidics in clinical diagnostics. Expert Rev Mol Diag 11:393–407. https://doi.org/10.1586/ERM.11.22
5. Sista R, Hua Z, Thwar P, Sudarsan A, Srinivasan V, Eckhardt A, Pollack M, Pamula V (2008) Development of a digital microfluidic platform for point of care testing. Lab Chip 8:2091–2104. https://doi.org/10.1039/b814922d
6. Gong J, Kim CJ (2008) Direct-referencing two-dimensional-array digital microfluidics using multilayer printed circuit board. J Microelectromech Syst 17:257–264. https://doi.org/10.1109/JMEMS.2007.912698
7. Malic L, Veres T, Tabrizian M (2009) Biochip functionalization using electrowetting-on-dielectric digital microfluidics for surface plasmon resonance imaging detection of DNA hybridization. Biosens Bioelectron 24:2218–2224. https://doi.org/10.1016/j.bios.2008.11.031
8. Nikapitiya NYJB, Nahar MM, Moon H (2017) Accurate, consistent, and fast droplet splitting and dispensing in electrowetting on dielectric digital microfluidics. Micro Nano Syst Lett 5:24. https://doi.org/10.1186/s40486-017-0058-6
9. Au SH, Kumar P, Wheeler AR (2011) A new angle on pluronic additives: advancing droplets and understanding in digital microfluidics. Langmuir 27:8586–8594. https://doi.org/10.1021/la201185c
10. Zhao Y, Chakrabarty K (2012) Cross-contamination avoidance for droplet routing in digital microfluidic biochips. IEEE Trans Comput Aided Des Integr Circuits Syst 31:817–830. https://doi.org/10.1109/TCAD.2012.2183369
11. Moon H, Cho SK, Garrell RL, Kim CJ (2002) Low voltage electrowetting-on-dielectric. J Appl Phys 92:4080–4087. https://doi.org/10.1063/1.1504171
12. Yi Z, Feng H, Zhou X, Shui L (2020) Design of an open electrowetting on dielectric device based on printed circuit board by using a parafilm M. Front Phys 8:193. https://doi.org/10.3389/fphy.2020.00193
13. Gu Z, Wu ML, Yan BY, Wang HF, Kong C (2020) Integrated digital microfluidic platform for colorimetric sensing of nitrite. ACS Omega 5:11196–11201. https://doi.org/10.1021/acsomega.0c01274
14. Newman S, Stephenson AP, Willsey M, Nguyen BH, Takahashi CN, Strauss K, Ceze L (2019) High density DNA data storage library via dehydration with digital microfluidic retrieval. Nat Commun 10:1706. https://doi.org/10.1038/s41467-019-09517-y
15. Lee KY, Park S, Lee YR, Chung SK (2016) Magnetic droplet microfluidic system incorporated with acoustic excitation for mixing enhancement. Sensor Actuators A Phys 243:59–65. https://doi.org/10.1016/j.sna.2016.03.009
16. Ren Y, Leung WWF (2013) Numerical and experimental investigation on flow and mixing in batch-mode centrifugal microfluidics. Int J Heat Mass Transf 60:95–104. https://doi.org/10.1016/j.ijheatmasstransfer.2012.12.023
17. Chang CC, Yang RJ (2007) Electrokinetic mixing in microfluidic systems. Microfluid Nanofluid 3:501–525. https://doi.org/10.1007/s10404-007-0178-z
18. Paik P, Pamula VK, Pollack MG, Fair RB (2003) Electrowetting-based droplet mixers for microfluidic systems. Lab Chip 3:28–33. https://doi.org/10.1039/b210825a
19. Sohrabi S, Kassir N, Moraveji MK (2020) Droplet microfluidics: fundamentals and its advanced applications. RSC Adv 10:27560–27574. https://doi.org/10.1039/d0ra04566g
20. Cooney CG, Chen CY, Emerling MR, Nadim A, Sterling JD (2006) Electrowetting droplet microfluidics on a single planar surface. Microfluid Nanofluid 2:435–446. https://doi.org/10.1007/s10404-006-0085-8
21. Mugele F, Baret JC, Steinhauser D (2006) Microfluidic mixing through electrowetting-induced droplet oscillations. Appl Phys Lett 88:204106. https://doi.org/10.1063/1.2204831
22. Mugele F, Staicu A, Bakker R, Van den ende D, (2011) Capillary stokes drift: a new driving mechanism for mixing in AC-electrowetting. Lab Chip 11:2011–2016. https://doi.org/10.1039/c0lc00702a
23. Shilton R, Tan MK, Yeo LY, Friend JR (2008) Particle concentration and mixing in microdrops driven by focused surface acoustic waves. J Appl Phys 104:014910. https://doi.org/10.1063/1.2951467
24. Alistar M, Gaudenz U (2017) Opendrop: an integrated do-it-yourself platform for personal use of biochips. Bioengineering 4:45. https://doi.org/10.3390/bioengineering4020045
25. Umapathi U, Chin S, Shin P, Koutentakis D, Ishii H (2018) Scaling electrowetting with printed circuit boards for large area droplet manipulation. MRS Adv 3:1475–1483. https://doi.org/10.1557/adv.2018.331
26. Won T, Jang D, Lee KY, Chung SK (2021) Acoustic bubble-induced microstreaming for biochemical droplet mixing enhancement in electrowetting (EW) microfluidic platforms. J Microelectromech Syst 30:783–790. https://doi.org/10.1109/JMEMS.2021.3103212
27. Kang KH (2002) How electrostatic fields change contact angle in electrowetting. Langmuir 18:10318–10322. https://doi.org/10.1021/la0263615
28. Fair RB (2007) Digital microfluidics: is a true lab-on-a-chip possible? Microfluid Nanofluid 3:245–281. https://doi.org/10.1007/s10404-007-0161-8
29. Quilliet C, Berge B (2001) Electrowetting: a recent outbreak. Curr Opin Colloid Interface Sci 6:34–39. https://doi.org/10.1016/S1359-0294(00)00085-6
30. Chen L, Bonaccurso E (2014) Electrowetting—from statics to dynamics. Adv Coll Interface Sci 210:2–12. https://doi.org/10.1016/j.cis.2013.09.007
31. Quinn A, Sedev R, Ralston J (2005) Contact angle saturation in electrowetting. J Phys Chem B 109:6268–6275. https://doi.org/10.1021/jp040478f

Publisher's Note